



OPEN ACCESS

EDITED BY
Chunyi Li,
Changchun University of Science
and Technology, China

REVIEWED BY
Yuan Tian,
Changchun University of Chinese
Medicine, China
Xiaoxiang Chen,
Nanjing Medical University, China

*CORRESPONDENCE
Jiandong Tai
taijd@jlu.edu.cn

SPECIALTY SECTION
This article was submitted to
Gastroenterology,
a section of the journal
Frontiers in Medicine

RECEIVED 12 July 2022
ACCEPTED 15 August 2022
PUBLISHED 15 September 2022

CITATION
Chen L, Yang F, Qi Z and Tai J (2022)
Predicting lymph node metastasis and
recurrence in patients with early stage
colorectal cancer.
Front. Med. 9:991785.
doi: 10.3389/fmed.2022.991785

COPYRIGHT
© 2022 Chen, Yang, Qi and Tai. This is
an open-access article distributed
under the terms of the [Creative
Commons Attribution License \(CC BY\)](https://creativecommons.org/licenses/by/4.0/).
The use, distribution or reproduction in
other forums is permitted, provided
the original author(s) and the copyright
owner(s) are credited and that the
original publication in this journal is
cited, in accordance with accepted
academic practice. No use, distribution
or reproduction is permitted which
does not comply with these terms.

Predicting lymph node metastasis and recurrence in patients with early stage colorectal cancer

Lei Chen¹, Funing Yang², Zhaoyan Qi¹ and Jiandong Tai^{1*}

¹Colorectal and Anal Surgery, General Surgery Center, First Hospital of Jilin University, Changchun, Jilin, China, ²Pediatric Outpatient Clinic, First Hospital of Jilin University, Changchun, Jilin, China

Tumor budding (TB), a powerful, independent predictor of colorectal cancer (CRC), is important for making appropriate treatment decisions. Currently, TB is assessed only using the tumor bud count (TBC). In this study, we aimed to develop a novel prediction model, which includes different TB features, for lymph node metastasis (LNM) and local recurrence in patients with pT1 CRC. Enrolled patients ($n = 354$) were stratified into training and validation cohorts. Independent predictors of LNM and recurrence were identified to generate predictive nomograms that were assessed using the area under the receiver operating characteristic (AUROC) and decision curve analysis (DCA). Seven LNM predictors [gross type, histological grade, lymphovascular invasion (LVI), stroma type, TBC, TB mitosis, and TB CDX2 expression] were identified in the training cohort. LNM, histology grade, LVI, TBC, stroma type, and TB mitosis were independent predictors of recurrence. We constructed an LNM predictive nomogram with a high clinical application value using the DCA. Additionally, a nomogram predicting recurrence-free survival (RFS) was constructed. It presented an AUROC value of 0.944 for the training cohort. These models may assist surgeons in making treatment decisions. In the high-risk group, radical surgery with a postoperative adjuvant chemotherapy was associated with RFS. Postoperative chemotherapy can be better for high-risk patients with pT1 CRC. We showed that TB features besides TBC play important roles in CRC pathogenesis, and our study provides prognostic information to guide the clinical management of patients with early stage CRC.

KEYWORDS

colorectal cancer, tumor budding, lymph node metastasis, predictive nomogram, recurrence-free survival, CDX2, risk stratification

Introduction

Owing to recent advances in diagnosis and treatment techniques, endoscopic resection has become the first choice of treatment for early stage colorectal cancer (CRC). However, the optimal management of such excisable tumors is still undefined because of potential metastases; thus, additional surgical resection is necessary to assess nodal status, but the frequency of lymph nodal metastasis (LNM) is relatively low (1). Previous studies have presented guidelines and proposed specific indicators for recommending completion surgery after endoscopic excision to prevent LNM or recurrence (2, 3). However, only approximately 10% (4–6) of patients who were referred for additional surgery based on these guidelines required it. Traditional pathological indicators are not sufficient to identify the need for additional surgery (7). Therefore, reliable criteria to assess patients requiring surgery are crucial.

Besides the resection margin, other promising indicators for additional surgical intervention include the tumor grade, lymphovascular invasion (LVI), and tumor budding (TB). The latter is characterized by the dissociation of small tumor complexes containing up to four cells that “bud” into the intratumoral or peritumoral stroma. TB is associated with a high risk of LNM in patients with pT1 CRC. Consequently, patients with pT1 CRC marked by prominent TB may benefit from additional surgical resection (8, 9). TB assessed in pre-operative biopsies could predict tumor regression for neo-adjuvant chemotherapy (10). Furthermore, high-level TB is a high-risk factor for patients with stage II CRC, and thus can warrant the consideration of adjuvant chemotherapy. Therefore, further studies are needed to determine whether TB assessments can help guide high-risk patients with pT1 CRC to undergo postoperative adjuvant chemotherapy to improve outcomes. The International Tumor Budding Consensus Conference (ITBCC) guidelines provide a standardized counting system for routine reporting. However, several factors should be considered when using the ITBCC TB scoring system in routine practice. First, the current ITBCC three-tier system (Bd1, Bd2, and Bd3) is the same for all stages of CRC. Both Bd2 and Bd3 are considered high-risk factors for LNM in pT1 CRC, whereas in stage II CRCs, only Bd3 is a risk factor for poor survival. Second, reporting of the absolute number of tumor buds is recommended, although inconsistency in tumor bud counts among pathologists may lead to differences in clinical management. Finally, the current TB assessment system focuses only on the tumor bud count and does not account for other features of TB, including structure, location, cell atypia, stroma type, tumor bud cell mitosis, and the immunohistochemical phenotype of the tumor bud cells. Including these other parameters in predictive models could improve the risk stratification power and prognostic value of TB and its various features.

In this retrospective study, we aimed to analyze the clinicopathologic characteristics to evaluate the risk stratification utility of TB features in early stage CRC. Furthermore, we developed a novel nomogram, including different characteristics of TB, to guide adjuvant chemotherapy in patients with early stage CRC. This approach could be combined with traditional clinicopathological indicators to assist surgeons in choosing the most suitable operation for patients with early stage CRC.

Materials and methods

Patients

This retrospective study included 354 consecutive patients who were pathologically diagnosed with pT1 CRC and who underwent radical surgery between January 2010 and December 2018 in the First Hospital of Jilin University (Changchun, China). Sixty patients received chemotherapy with fluorouracil plus oxaliplatin after surgery. We excluded patients who (i) underwent only endoscopic excision; (ii) with missing follow-up data; (iii) with specific histological subtypes of adenocarcinomas, such as poorly cohesive carcinoma, signet-ring cell carcinoma, micropapillary adenocarcinoma, mucinous adenocarcinoma, and medullary adenocarcinoma; and (iv) with more complicated or advanced CRC, higher than stage T1. The study protocol was approved by the institutional ethics committee of Jilin University First Hospital. The need for written informed consent was waived because of the retrospective nature of the study.

Histology

Hematoxylin and eosin-stained slides were reviewed by two pathologists. All slides were reviewed in a double-blinded manner, without knowledge of the corresponding pathological diagnoses. The initial clinical and pathological stages of the disease in all patients were revised according to the American Joint Committee on Cancer staging system (eighth edition). Histological type and grade were defined according to the latest World Health Organization classification system. In all specimens, the following histological features were evaluated: the LVI, predominant structure of tumor bud (cluster or single-cell), predominant location of TB (peritumoral or intratumoral budding), and tumor bud cell atypia (non-specific or anaplasia-like; anaplasia was defined as any $\times 400$ magnification field with ≥ 3 nuclei with diameters equal to or greater than 5 lymphocyte nuclei) (11), stroma type (inflammatory, fibrotic, or myxoid; the predominant feature was recorded), mitosis in tumor bud cells, and tumor bud count. TB was defined as the dissociation

of small tumor complexes containing more than five cells that “budded” into the intratumoral or peritumoral stroma. TB was scored by two independent pathologists according to the ITBCC guidelines (12). Hematoxylin and eosin-stained sections were evaluated at medium magnification ($\times 10$) to determine the densest area of TB at the invasive tumor front (“hotspot”). To reduce interobserver variability, TB features were independently evaluated by two single-blinded pathologists. The final classification of TB features was determined based on agreement among at least two pathologists.

Immunohistochemistry

Immunohistochemistry was performed as described previously (13). Tissue sections were stained using the following primary antibodies: rabbit monoclonal CDX2 (EP25; Zhongshan Golden Bridge Biotechnology LLC, Beijing, China; ready-to-use); Ki-67 (30-9; Ventana, Tucson, AZ, United States; ready-to-use), epidermal growth factor receptor (EGFR; EP22; Zhongshan Golden Bridge Biotechnology LLC; ready-to-use), p53 (4A4 + UMAB4; Zhongshan Golden Bridge Biotechnology LLC; ready-to-use), BRAF V600E (VE1; Ventana; ready-to-use), and microsatellite instability (MSI) proteins, including MLH1 (ES05), PMS2 (EP51), MSH2 (RED2), and MSH6 (EP49) (Zhongshan Golden Bridge Biotechnology LLC; ready-to-use).

CDX2 and EGFR immunohistochemical staining were performed as described previously (14). The extent of tumor bed cell staining (0–100%) and the staining intensity (0, negative; 1, weak brown; 2, brown; and 3, dark brown) were evaluated. The final scores were defined as the product of the extent and intensity scores. Next, each case was scored as high or low, using the median final score as the cut-off point for the following test. The immunohistochemical staining patterns of p53 were classified into two subgroups: (a) wild-type pattern, indicated by scattered nuclear staining in tumor cells, and (b) mutant-type pattern, in which the majority of tumor cells ($> 60\%$) showed diffuse strong nuclear positivity or were completely devoid of any staining. Only staining for the expression of cytoplasmic BRAF V600E was considered positive. The MSI status was classified into two subgroups: (a) MSI-high, if any one of the four mismatch repair proteins (MLH1, PMS2, MSH2, and MSH6) was nuclear negative in all tumor cells, but positive in internal controls; and (b) MSI-low, if all four mismatch repair proteins were positive in cancer cells. The p53- and BRAF-staining patterns and MSI status were reported by two single-blinded observers.

Statistical analysis

The clinicopathological findings of the CRC specimens were compared using the chi-square or Fisher’s exact test for

categorical variables. The non-parametric Mann–Whitney *U* test was used to analyze age, Ki67 labeling index, and TBC datasets because of their non-normal distribution.

Multivariate logistic and Cox regression analyses were used to identify significant independent factors for predicting LNM or recurrence-free survival (RFS). Variables with $P < 0.1$ in the univariate analysis were included in the multivariate analysis model. The RFS of the patients was analyzed using the Kaplan–Meier method and log-rank test. *P* values were obtained using two-tailed statistical analyses, and the significance level was set at 5% ($P < 0.05$). R software (version 4.1.0¹) was used for all statistical analyses. The R statistical packages “rms,” “barplot,” “survival,” “Hmisc,” “MASS,” and “pROC” were used to plot the distribution of risk scores and recurrence or distant metastasis, plot calibration, generate receiver operating characteristic curve, build a nomogram, and draw Kaplan–Meier curves. The package “rmda” was used to draw the decision curve analysis (DCA) curves, and “forestplot” was used to draw the forest plot.

Results

Demographic and clinicopathological findings

The baseline clinicopathological characteristics of the participants ($n = 354$) are summarized in **Table 1**. LNM was present in 49 (13.8%) patients (mean age \pm standard deviation = 65.2 ± 10.3 years; range = 30–91 years). Recurrence was observed in 38 (10.7%) patients, and the follow-up period was 37.4 ± 16.3 months (range = 14.2–59.9 months).

Evaluation and validation of the lymph node metastasis predictive nomogram

In total, 354 patients were included and randomly allocated to a training cohort ($n = 234$) and validation cohort ($n = 120$) at a ratio of approximately 2–1 based on the data splitting approach. Based on the univariate logistic regression analysis results of the training cohort, seven factors, namely general tumor type, histology grade (**Figure 1A**), LVI (**Figure 1B**), tumor bud stroma (**Figures 1C,D**), tumor bud count, tumor bud cell mitosis (**Figure 1E**), and CDX2 expression (**Figure 1F**), were linked to the LNM status (**Figure 2A**).

General tumor type [pedunculated vs. non-pedunculated; odds ratio (OR) = 0.641; 95% confidence interval (CI) = 0.098–4.185], histological grade (high-grade vs. low-grade; OR = 5.561;

¹ www.r-project.org

TABLE 1 Demographics of surgery of 354 patients with pT1 CRC who underwent surgical resection.

Variable		All patients
Age (years)*		65.2 ± 10.3 [30–91]
Sex	Female	131 (37.0%)
	Male	223 (63.0%)
LNM	Absent	305 (86.2%)
	Present	49 (13.8%)
Gross tumor type	Non-pedunculated	161 (45.5%)
	Pedunculated	193 (54.5%)
TP53	Wild-type	27 (7.6%)
	Mutant-type	156 (44.1%)
	-	171 (48.3%)
MSI	MSI-high	11 (3.1%)
	MSI-low	172 (48.6%)
	-	171 (48.3%)
BRAF	Absent	182 (51.4%)
	Present	1 (0.3%)
	-	171 (48.3%)
Ki67 (%)*		78.7 ± 13.2 [5.0–95.0]
Histology grade	Low-grade	339 (95.8%)
	High-grade	15 (4.2%)
Lymph-vascular invasion	Absent	315 (89.0%)
	Present	39 (11.0%)
TB construction	Cluster	201 (56.8%)
	Single	153 (43.2%)
TB location	ITB	118 (33.4%)
	PTB	236 (66.7%)
TB atypia	Non-specific	311 (87.9%)
	Anaplasia-like	43 (12.1%)
TB stroma	Inflammation	100 (28.3%)
	Fibrosis	192 (54.2%)
	Myxoid	62 (17.5%)
TB mitosis	Absent	298 (84.2%)
	Present	56 (15.8%)
TB quantity*		10.7 ± 3.7 [0.0–18.0]
TB CDX2 status	Negative	87 (24.6%)
	Positive	267 (75.4%)
TB EGFR status	Negative	50 (14.1%)
	Positive	304 (85.9%)
Recurrence	Absent	316 (89.3%)
	Present	38 (10.7%)

*Data are mean ± standard deviation. MSI, microsatellite instability; TB, tumor budding.

95% CI = 1.933–16.003), LVI (present vs. absent; OR = 34.194; 95% CI = 9.511–122.930), tumor bud cell stroma type (myxoid vs. inflammatory; OR = 6.746; 95% CI = 1.831–24.851), tumor bud count (high vs. low; OR = 63.429; 95% CI = 14.623–275.130), TB mitosis (present vs. absent; OR = 2.770; 95% CI = 0.643–11.925), and TB CDX2 expression status (negative vs. positive; OR = 15.919; 95% CI = 4.259–59.494) were

independent predictors of recurrence in the multivariate analyses (Table 2 and Figure 2B).

The calibration curve of the LNM nomogram was highly consistent with the standard curve, indicating the high reliability of the predictive ability of the nomogram (Figures 2C,D). The DCA curves for the developed LNM nomogram (Figure 2E) and tumor bud count (Figure 2F) in the training and validation cohorts indicated that the DCA of the predictive nomogram had higher net benefits than the tumor bud count, indicating higher clinical application value.

Evaluation and validation of the recurrence-free survival prediction nomogram

Cox univariate and multivariate regression analyses were performed in the training cohort to identify the variables for building the RFS predictive nomogram. RFS was significantly associated with LNM, general tumor type, histology grade, LVI, stroma type, tumor bud count, tumor bud cell mitosis, and CDX2 expression status (Figure 3A). In the multivariate Cox proportional hazards model, LNM, histology grade, LVI, TBC, stroma type, and TB mitosis were independent predictors of local recurrence (Table 3). These variables were used to build a predictive nomogram for RFS (Figure 3B). Calibration curves based on the six variables are shown in Figures 3C,D. There was a positive agreement between the nomogram-predicted and actual probabilities of 5-year RFS in the training and validation cohorts, respectively. The predictive ability of the RFS nomogram was evaluated by analyzing the area under the ROC (AUROC). The nomograms displayed discriminatory power in predicting the postoperative RFS in the training cohort. The C-indices of the RFS nomogram and tumor bud count were 0.944 (95% CI = 0.934–0.952) and 0.689 (95% CI = 0.642–0.736), respectively (Figures 3E,F).

Based on the nomogram score, patients were stratified into low- (score ≤ 160) and high-risk (score > 160) for recurrence and mortality, respectively. We used Kaplan–Meier curves and the log-rank test to analyze RFS in patients with pT1 CRC after stratification (low-risk vs. high-risk) using the nomogram ($p < 0.001$; Figure 4A). In the high-risk group, patients who only underwent radical surgery had a lower RFS ($p = 0.029$; Figure 4B), compared to that of patients who underwent radical surgery and a postoperative chemotherapy.

Discussion

Although the traditional TNM staging system remains essential for risk stratification in patients with CRC, the heterogeneity in survival rates within the same stages indicates the need for additional prognostic biomarkers. Furthermore, the

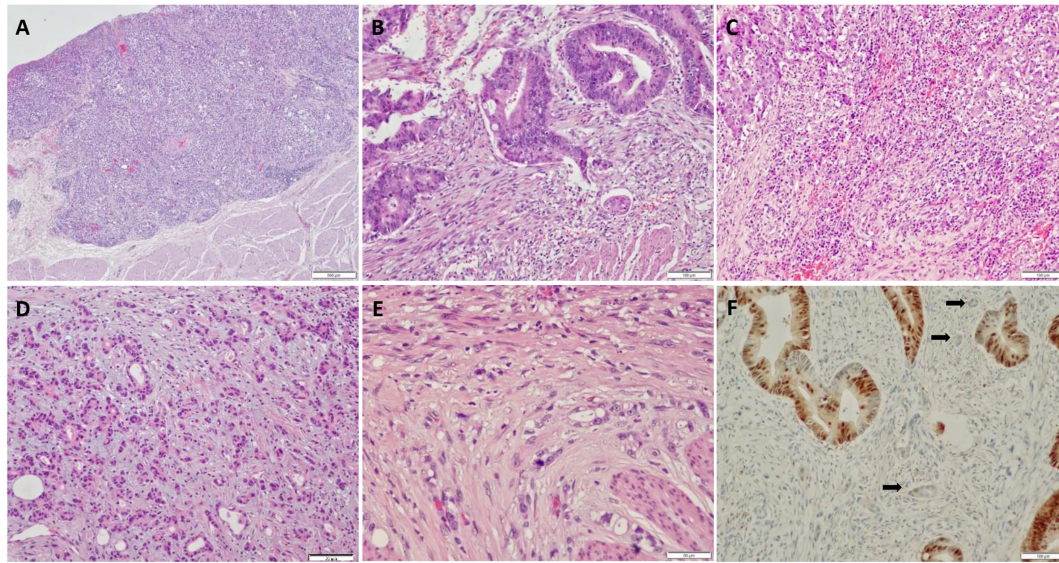


FIGURE 1
 Histological and immunohistochemical features of pT1 colorectal cancer (CRC). **(A)** High histology grade; **(B)** lymph-vascular invasion observed in a biopsy specimen; **(C)** inflammatory stroma surrounding tumor budding (TB); **(D)** myxoid stroma surrounding TB; **(E)** mitosis present in TB; **(F)** CDX2 expression in tumor cells, while loss of expression in TB.

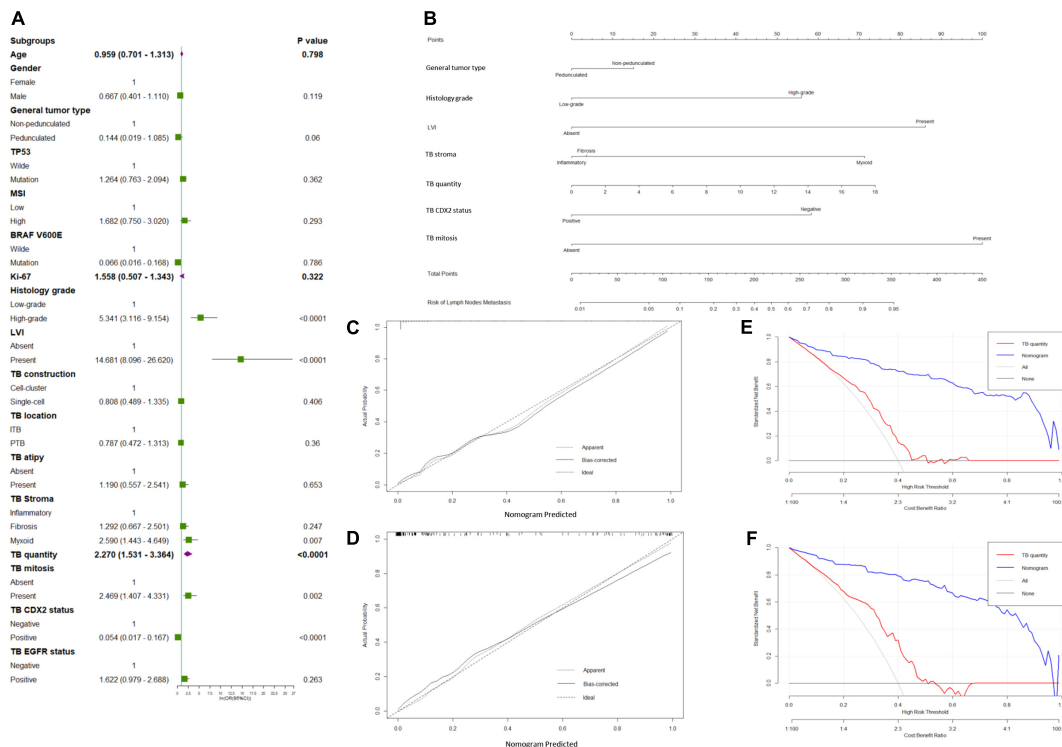


FIGURE 2
 Predicted model of lymph node metastasis (LNM). **(A)** Forest plots to decipher the risk factors associated with LNM identified in the univariate logistic regression analysis; **(B)** newly developed nomogram for predicting LNM in patients with pT1 CRC. The calibration curve for predicting LNM of pT1 CRCs in the **(C)** training and **(D)** validation cohorts. Decision curve analysis of the nomogram and TB quantity alone for predicting LNM in patients with pT1 CRC in the **(E)** training cohort and **(F)** validation cohort.

TABLE 2 Multivariate logistic regression analysis of lymph node metastasis.

	Training cohort (n = 234)		Validation cohort (n = 120)	
	OR (95% CI)	P-value	OR (95% CI)	P-value
Gross tumor type				
Non-pedunculated	1.000		1.000	
Pedunculated	0.641 (0.098–4.185)	0.477	0.826 (0.124–4.079)	0.772
Histology grade				
Low-grade	1.000		1.000	
High-grade	5.561 (1.933–16.003)	0.002	4.403 (1.046–18.520)	0.043
LVI				
Absent	1.000		1.000	
Present	34.194 (9.511–122.930)	0.004	11.156 (2.186–56.912)	0.003
TB stroma				
Inflammation	1.000		1.000	
Fibrosis	1.667 (1.278–9.451)	0.527	1.206 (1.1412–6.216)	0.087
Myxoid	6.746 (1.831–24.851)	0.032	4.303 (1.945–15.933)	0.022
TB mitosis				
Absent	1.000		1.000	
Present	2.770 (0.643–11.925)	0.171	1.013 (0.926–2.618)	0.568
TB quantity	63.429 (14.623–275.130)	0.001	28.952 (4.010–208.990)	0.008
TB CDX2 status				
Negative	15.919 (4.259–59.494)	0.021	17.350 (7.689–25.778)	0.003
Positive	1.000		1.000	

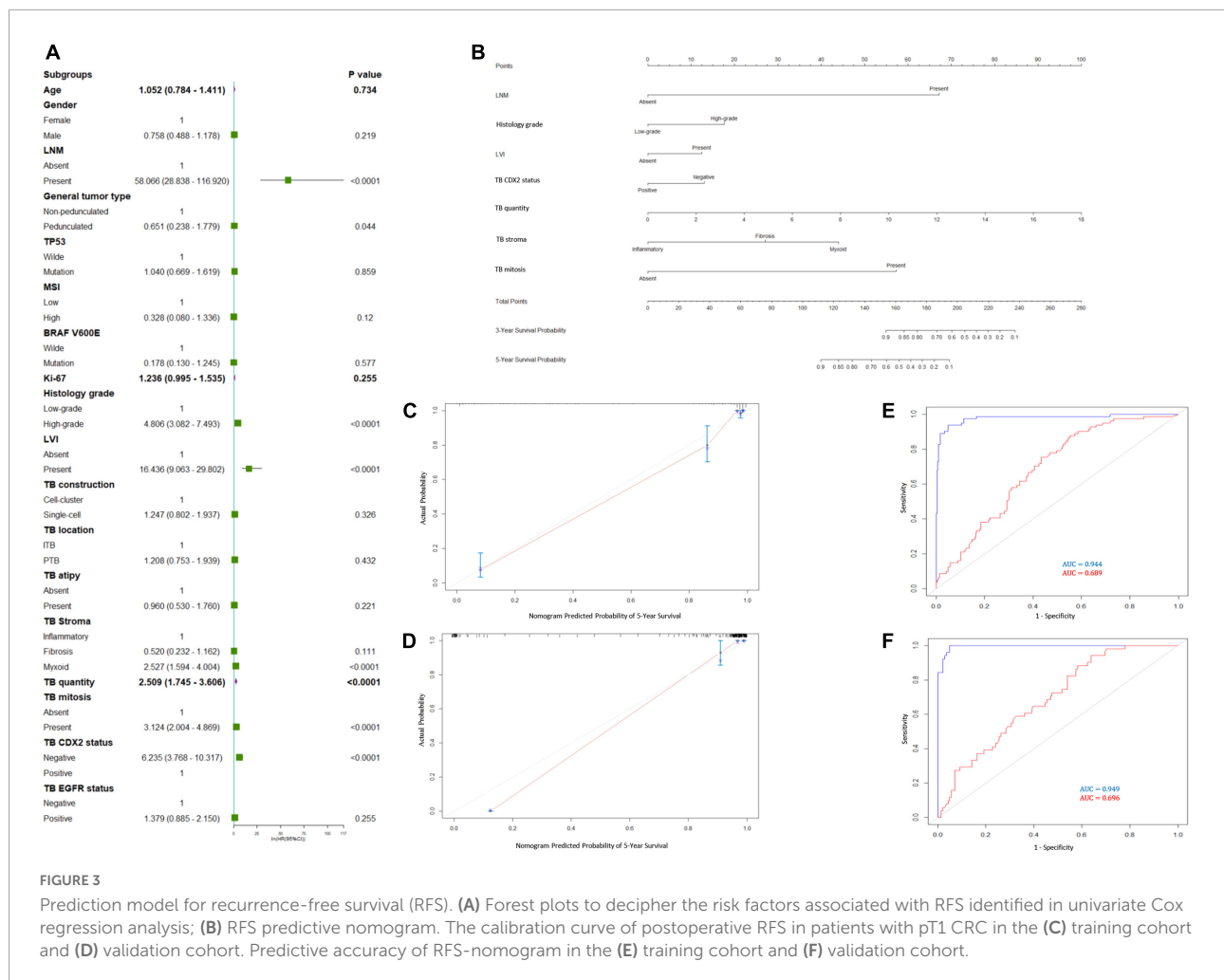
CI, confidence interval; OR, odds ratio; MSI, microsatellite instability; LVI, lymphovascular invasion; TB, tumor budding.

invasive front morphology may be more representative of the biological behavior of the tumor than the primary tumor core morphology (15). Our study demonstrated that the morphology and immunohistochemical features of TB in cases of early stage CRC were predictive of tumor progression and local recurrence. Among the various features, non-pedunculated gross type, high histological grade, LVI, myxoid-type tumor bud stroma, high tumor bud count, TB mitosis, and loss of CDX2 expression were independent predictors of LNM, whereas LNM, histology grade, LVI, TBC, stroma type, and TB mitosis were independent predictors of local recurrence in patients with pT1 CRC.

TB is a morphological characteristic that reflects the high aggressiveness of tumors at the invasion margin. A previous study revealed that high-level TB correlated with mutated KRAS or MSS/pMMR (16). Furthermore, patients with CRC who have a KRAS mutation and MSS/pMMR tumor were part of a group with the poorest prognosis (17). It is defined as a morphologic surrogate of epithelial-mesenchymal transition (EMT), a mechanism through which tumor cells acquire motility and invasiveness (18). EMT facilitates the detachment of cancer cells from the tumor mass and their subsequent infiltration in the extracellular matrix as single cells or small clusters (1, 9). TB has a strong risk stratification utility, so much so that the ITBCC system can reliably predict the

prognosis of patients with CRC based on tumor bud count alone (19). However, not all patients with a high tumor bud count will have a poor prognosis; thus, further investigation of the characteristics of TB could improve its value for risk stratification. Our study is the first to improve the current ITBCC system by exploring various features of TB to predict LNM in patients with pT1 CRC, rather than limiting the input parameters to the tumor bud count. Moreover, the nomograms that we developed showed stronger discriminative ability than tumor bud count in predicting LNM or local recurrence. Thus, our easy-to-use predictive nomograms could be useful tools to quantify the probability of RFS.

A high histological grade has also been shown to be associated with aggressive tumor biology and to be of prognostic significance; it has been associated with various informative tumor parameters in human malignancies (20–25). Our results agree with the findings of previous studies on non-CRCs and indicate that a high histological grade is of prognostic value for pT1 CRC. Additionally, we focused on the presence of atypia of tumor bud cells, but it was not of statistical significance; it was mainly present in the tumor center. Furthermore, tumor bud cell mitosis was observed in 15.8% of the cases in the present study. Mitosis results from rapid cell proliferation and is correlated with tumor proliferation and invasiveness; it is associated with



adverse clinical outcomes in other cancer types (26), although its prognostic value in CRC has not yet been defined. A previous study revealed that a decrease in mitosis is associated with high-level TB (27), which may represent the potential decrease in the mitosis of tumor bud cells because of fibroblastic cells around TB during the EMT process in an effort to slow down tumor invasion. Thus, mitosis in TB may reflect tumor biology and may provide valuable prognostic information.

Unlike the tumor core, the environment at the tumor front is not static; inflammatory, fibrotic, and myxoid stroma are histologic features representing snapshots of the dynamic process of extracellular matrix remodeling. The immature or myxoid stroma desmoplastic reaction has been recognized as an independent prognostic predictor in CRC (28). This feature, however, has not been routinely adopted in pathology reports for clinical care. Furthermore, myxoid stroma is associated with the absence of tumor-infiltrating lymphocytes in CRC (29), which enhance tumor immune escape. Some studies have demonstrated that the immature myxoid stroma is associated with a high degree of tumor budding (30). The myxoid stroma

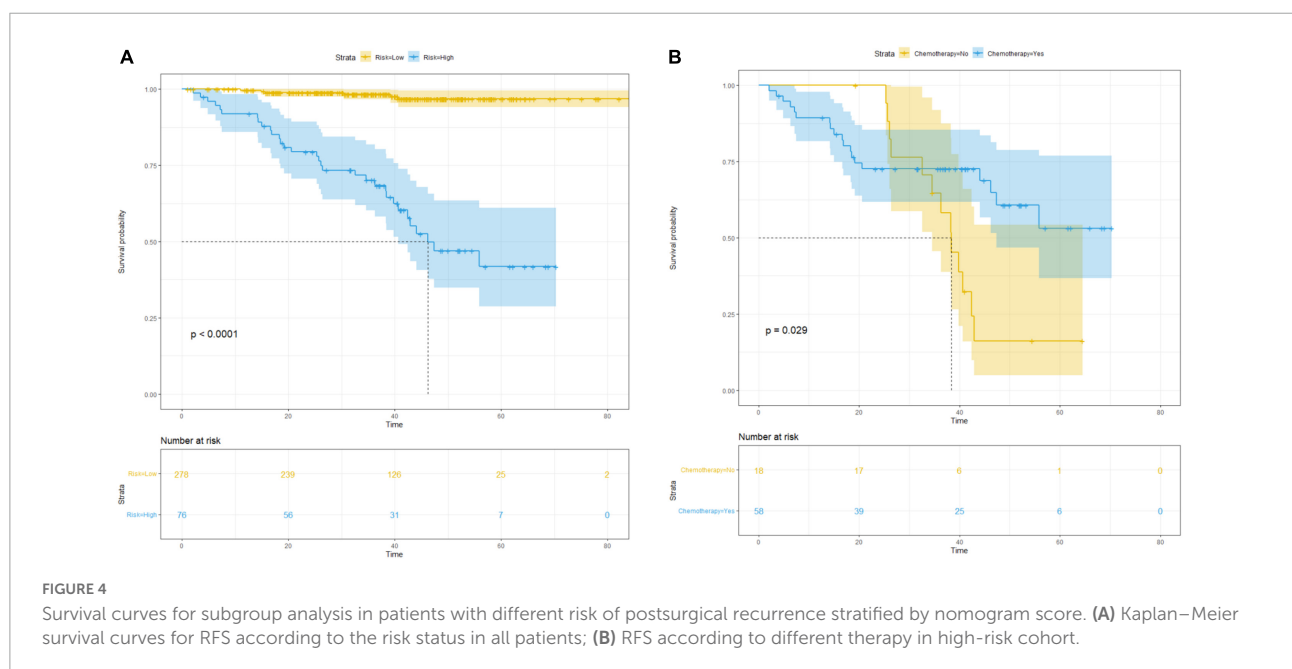
surrounding the tumor buds that appear at the tumor front is regarded as an immature stroma with a high potential to disseminate and metastasize (31). Consistent with the findings of a previous study (32), in the current study, myxoid stroma was significantly associated with the presence of LNM and local recurrence in patients with pT1 CRC.

In addition to the histological characteristics of TB, we also investigated the immunophenotype of TB. We observed a loss of CDX2 expression in 6.6% of tumor buds, which differed from the tumor core. Notably, CDX2 inhibits EMT and metastasis of CRC by regulating Snail and β -catenin expression (33). CDX2, an intestine-specific transcription factor, has been strongly implicated in the development of the intestinal mucosa (34). Emerging evidence suggests the crucial role of CDX2 as a tumor suppressor during colorectal carcinogenesis. CDX2 expression is inversely associated with tumor grade in CRC (35, 36). Consistent with the findings of a previous study, the downregulation of CDX2 expression was associated with LNM in patients with pT1 CRC. The lack of CDX2 expression in tumor buds may indicate that they are in a

TABLE 3 Multivariate COX regression analysis of recurrence.

	Training cohort (n = 234)		Validation cohort (n = 120)	
	HR (95% CI)	P-value	HR (95% CI)	P-value
LNM				
Absent	1.000		1.000	
Present	32.292 (14.401–72.407)	< 0.0001	16.331 (6.007–58.260)	< 0.0001
Gross tumor type				
Non-pedunculated	1.000		1.000	
Pedunculated	0.733 (0.171–2.153)	0.337	0.891 (0.432–3.014)	0.547
Histology grade				
Low-grade	1.000		1.000	
High-grade	1.622 (1.002–2.627)	0.049	1.548 (0.771–3.107)	0.218
LVI				
Absent	1.000		1.000	
Present	2.686 (1.162–6.208)	0.021	2.958 (1.160–7.541)	0.023
TB stroma				
Inflammation	1.000		1.000	
Fibrosis	1.256 (0.449–1.632)	0.551	1.192 (0.312–1.880)	0.715
Myxoid	1.719 (0.264–1.955)	0.001	1.280 (0.950–2.819)	0.151
TB mitosis				
Absent	1.000		1.000	
Present	1.022 (0.540–1.933)	< 0.0001	1.567 (0.615–2.673)	0.094
TB quantity	1.703 (1.055–2.750)	0.029	1.563 (0.838–2.914)	0.020
TB CDX2 status				
Negative	0.935 (0.520–1.679)	0.216	1.789 (0.711–4.502)	0.799
Positive	1.000		1.000	

Statistical analyses were conducted using log-rank tests and a Cox proportional hazards model. CI, confidence interval; LVI, lymphovascular invasion; RFS, recurrence-free survival; TB, tumor budding.



state of EMT; thus, it could predict poor prognosis in patients with CRC. Moreover, because these features are associated with LNM, they can be applied to endoscopic biopsy specimens to better predict tumor progression behavior. To the best of our knowledge, these findings have not been previously reported. Additional studies with larger cohorts are required to validate the prognostic implications of the histological and immunohistochemical features of TB that may help predict the prognosis or occurrence of LNM.

Our novel nomogram can effectively stratify the recurrence risk in pT1 CRC patients, and the KM survival curve shows that the RFS of high-risk patients is much shorter than that of the low-risk. Furthermore, our data revealed that adjuvant chemotherapy is necessary in the high-risk group. Therefore, adjuvant chemotherapy is recommended for high-risk patients even if they do not have LNM. Our method could be applied to determine risk stratification strategies for patients with pT1 CRC; for example, to identify low-risk patients to avoid unnecessary additional treatment, while identifying high-risk patients to enable timely and effective treatment. Low-risk patients could extend their follow-up periods, improving their quality of life and reducing postoperative complications and financial costs. However, this study had some limitations. First, the statistical power was limited because this was a single-center retrospective study. Second, owing to the retrospective study design, potential selection biases could not be ruled out. Finally, although the study focused on identifying the most significant predictors of LNM and local recurrence, it is unclear whether these findings can be generalized.

In conclusion, tumor bud count and other features of TB are associated with LNM and poor prognosis in patients with pT1CRC. Although tumor bud count, stroma type, and the CDX2 expression status in tumor buds were identified as risk factors for LNM, only tumor bud count was significantly correlated with local recurrence in patients with pT1 CRC. Thus, these features of TB should be incorporated into the routine evaluation of CRC, as they may provide valuable information to guide clinical therapy. Additional studies in a multi-institutional setting are needed to confirm these findings.

References

- Cappellesso R, Luchini C, Veronese N, Lo Mele M, Rosa-Rizzotto E, Guido E, et al. Tumor budding as a risk factor for nodal metastasis in pT1 colorectal cancers: a meta-analysis. *Hum Pathol.* (2017) 65:62–70. doi: 10.1016/j.humpath.2017.04.013
- Watanabe T, Muro K, Ajioka Y, Hashiguchi Y, Ito Y, Saito Y, et al. Japanese society for cancer of the colon and rectum (JSCCR) guidelines 2016 for the treatment of colorectal cancer. *Int J Clin Oncol.* (2018) 23:1–34. doi: 10.1007/s10147-017-1101-6
- Benson AB, Venook AP, Al-Hawary MM, Cederquist L, Chen YJ, Ciombor KK, et al. Rectal cancer, version 2.2018, NCCN clinical practice guidelines in oncology. *J Natl Compr Cancer Netw.* (2018) 16:874–901. doi: 10.6004/jnccn.2018.0061
- Ichimasa K, Kudo SE, Mori Y, Misawa M, Matsudaira S, Kouyama Y, et al. Artificial intelligence may help in predicting the need for additional surgery after endoscopic resection of T1 colorectal cancer. *Endoscopy.* (2018) 50:230–40. doi: 10.1055/s-0043-122385
- Yamashita K, Oka S. Preceding endoscopic submucosal dissection for T1 colorectal carcinoma does not affect the prognosis of patients who underwent additional surgery: a large multicenter propensity score-matched analysis. *J Gastroenterol.* (2019) 54:897–906. doi: 10.1007/s00535-019-01590-w
- Overwater A, Kessels K, Elias SG, Backes Y, Spanier BWM, Seerden TCJ, et al. Endoscopic resection of high-risk T1 colorectal carcinoma prior to surgical

Data availability statement

The original contributions presented in this study are included in the article/supplementary material, further inquiries can be directed to the corresponding author.

Author contributions

LC and JT performed the material preparation and data collection and analysis. LC wrote the first draft of the manuscript. All authors contributed to the article and approved the submitted version.

Funding

This research was partially funded by the “Intestinal flora alleviates the cumulative effect of heavy metal pollutants on colorectal cancer project” of Jilin Provincial Finance Department (JLSCZT2019-018).

Conflict of interest

The authors declare that the research was conducted in the absence of any commercial or financial relationships that could be construed as a potential conflict of interest.

Publisher's note

All claims expressed in this article are solely those of the authors and do not necessarily represent those of their affiliated organizations, or those of the publisher, the editors and the reviewers. Any product that may be evaluated in this article, or claim that may be made by its manufacturer, is not guaranteed or endorsed by the publisher.

- resection has no adverse effect on long-term outcomes. *Gut*. (2018) 67:284–90. doi: 10.1136/gutjnl-2015-310961
7. Steele RJ, Pox C, Kuipers EJ, Minoli G, Lambert R. European guidelines for quality assurance in colorectal cancer screening and diagnosis. first edition—management of lesions detected in colorectal cancer screening. *Endoscopy*. (2012) 44(Suppl. 3):Se140–50. doi: 10.1055/s-0032-1309802
8. Okamura T, Shimada Y, Nogami H, Kameyama H, Kobayashi T, Kosugi S, et al. Tumor budding detection by immunohistochemical staining is not superior to hematoxylin and eosin staining for predicting lymph node metastasis in pT1 colorectal cancer. *Dis Colon Rectum*. (2016) 59:396–402. doi: 10.1097/dcr.0000000000000567
9. Koelzer VH, Zlobec I, Lugli A. Tumor budding in colorectal cancer—ready for diagnostic practice? *Hum Pathol*. (2016) 47:4–19. doi: 10.1016/j.humpath.2015.08.007
10. Rogers AC, Gibbons D, Hanly AM, Hyland JM, O'Connell PR, Winter DC, et al. Prognostic significance of tumor budding in rectal cancer biopsies before neoadjuvant therapy. *Mod Pathol*. (2014) 27:156–62. doi: 10.1038/modpathol.2013.124
11. Lewis JS Jr., Scantlebury JB, Luo J, Thorstad WL. Tumor cell anaplasia and multinucleation are predictors of disease recurrence in oropharyngeal squamous cell carcinoma, including among just the human papillomavirus-related cancers. *Am J Surg Pathol*. (2012) 36:1036–46. doi: 10.1097/PAS.0b013e3182583678
12. Lugli A, Kirsch R, Ajioka Y, Bosman F, Cathomas G, Dawson H, et al. Recommendations for reporting tumor budding in colorectal cancer based on the International tumor budding consensus conference (ITBCC) 2016. *Mod Pathol*. (2017) 30:1299–311. doi: 10.1038/modpathol.2017.46
13. Cao L, Wang Z, Duan L, Wei L. Analysis of endoscopy findings to identify early gastric cancers with tumor budding: a retrospective study. *J Gastrointest Surg*. (2020) 25:1706–15. doi: 10.1007/s11605-020-04862-6
14. Yu J, Liu D, Sun X, Yang K, Yao J, Cheng C, et al. CDX2 inhibits the proliferation and tumor formation of colon cancer cells by suppressing Wnt/ β -catenin signaling via transactivation of GSK-3 β and Axin2 expression. *Cell Death Dis*. (2019) 10:26. doi: 10.1038/s41419-018-1263-9
15. Quail DF, Joyce JA. Microenvironmental regulation of tumor progression and metastasis. *Nat Med*. (2013) 19:1423–37. doi: 10.1038/nm.3394
16. Hatthakarnkul P, Quinn JA, Matly AAM, Ammar A, van Wyk HC, McMillan DC, et al. Systematic review of tumour budding and association with common mutations in patients with colorectal cancer. *Crit Rev Oncol Hematol*. (2021) 167:103490. doi: 10.1016/j.critrevonc.2021.103490
17. Sinicrope FA, Shi Q, Smyrk TC, Thibodeau SN, Dienstmann R, Guinney J, et al. Molecular markers identify subtypes of stage III colon cancer associated with patient outcomes. *Gastroenterology*. (2015) 148:88–99. doi: 10.1053/j.gastro.2014.09.041
18. Dawson H, Lugli A. Molecular and pathogenetic aspects of tumor budding in colorectal cancer. *Front Med*. (2015) 2:11. doi: 10.3389/fmed.2015.00011
19. Dawson H, Galuppini F, Träger P, Berger MD, Studer P, Brügger L, et al. Validation of the International tumor budding consensus conference 2016 recommendations on tumor budding in stage I-IV colorectal cancer. *Hum Pathol*. (2019) 85:145–51. doi: 10.1016/j.humpath.2018.10.023
20. Thomas JS, Kerr GR, Jack WJ, Campbell F, McKay L, Pedersen HC, et al. Histological grading of invasive breast carcinoma—a simplification of existing methods in a large conservation series with long-term follow-up. *Histopathology*. (2009) 55:724–31. doi: 10.1111/j.1365-2559.2009.03429.x
21. Nakazato Y, Minami Y, Kobayashi H, Satomi K, Anami Y, Tsuta K, et al. Nuclear grading of primary pulmonary adenocarcinomas: correlation between nuclear size and prognosis. *Cancer*. (2010) 116:2011–9. doi: 10.1002/cncr.24948
22. Kadota K, Suzuki K, Colovos C, Sima CS, Rusch VW, Travis WD, et al. A nuclear grading system is a strong predictor of survival in epitheloid diffuse malignant pleural mesothelioma. *Mod Pathol*. (2012) 25:260–71. doi: 10.1038/modpathol.2011.146
23. Genega EM, Kapali M, Torres-Quinones M, Huang WC, Knauss JS, Wang LP, et al. Impact of the 1998 World Health Organization/International society of urological pathology classification system for urothelial neoplasms of the kidney. *Mod Pathol*. (2005) 18:11–8. doi: 10.1038/modpathol.3800268
24. Lipponen PK, Eskelinen MJ, Jauhiainen K, Harju E, Terho R, Haapasalo H. Independent clinical, histological and quantitative prognostic factors in transitional-cell bladder tumours, with special reference to mitotic frequency. *Int J Cancer*. (1992) 51:396–403. doi: 10.1002/ijc.2910510311
25. Veltri RW, Christudass CS, Isharwal S. Nuclear morphometry, nucleomics and prostate cancer progression. *Asian J Androl*. (2012) 14:375–84. doi: 10.1038/aja.2011.148
26. Nakaguro M, Sato Y, Tada Y, Kawakita D, Hirai H, Urano M, et al. Prognostic implication of histopathologic indicators in salivary duct carcinoma: proposal of a novel histologic risk stratification model. *Am J Surg Pathol*. (2020) 44:526–35. doi: 10.1097/pas.0000000000001413
27. Hacking S, Sajjan S, Angert M, Ebare K, Jin C, Chavarria H, et al. Tumor budding in colorectal carcinoma showing a paradoxical mitotic index (Via PHH3) with possible association to the tumor stromal microenvironment. *Appl Immunohistochem Mol Morphol*. (2020) 28:627–34. doi: 10.1097/pai.0000000000000805
28. Ueno H, Kanemitsu Y, Sekine S, Ishiguro M, Ito E, Hashiguchi Y, et al. Desmoplastic pattern at the tumor front defines poor-prognosis subtypes of colorectal cancer. *Am J Surg Pathol*. (2017) 41:1506–12. doi: 10.1097/pas.0000000000000946
29. González IA, Bauer PS, Liu J, Chatterjee D. Intraepithelial tumour infiltrating lymphocytes are associated with absence of tumour budding and immature/myxoid desmoplastic reaction, and with better recurrence-free survival in stages I-III colorectal cancer. *Histopathology*. (2021) 78:252–64. doi: 10.1111/his.14211
30. Cao L, Sun PL. Desmoplastic reaction and tumor budding in cervical squamous cell carcinoma are prognostic factors for distant metastasis: a retrospective study. *Cancer Manage Res*. (2020) 12:137–44. doi: 10.2147/cmar.s231356
31. Kalluri R, Zeisberg M. Fibroblasts in cancer. *Nat Rev Cancer*. (2006) 6:582–98. doi: 10.1038/nrc1877
32. Ueno H, Kanemitsu Y, Sekine S, Ishiguro M, Ito E, Hashiguchi Y, et al. A multicenter study of the prognostic value of desmoplastic reaction categorization in stage II colorectal cancer. *Am J Surg Pathol*. (2019) 43:1015–22. doi: 10.1097/pas.0000000000001272
33. Yu J, Li S, Xu Z, Guo J, Li X, Wu Y, et al. CDX2 inhibits epithelial-mesenchymal transition in colorectal cancer by modulation of snail expression and β -catenin stabilisation via transactivation of PTEN expression. *Br J Cancer*. (2021) 124:270–80. doi: 10.1038/s41416-020-01148-1
34. Grainger S, Savory JG, Lohnes D. Cdx2 regulates patterning of the intestinal epithelium. *Dev Biol*. (2010) 339:155–65. doi: 10.1016/j.ydbio.2009.12.025
35. Baba Y, Noshio K, Shima K, Freed E, Irahara N, Philips J, et al. Relationship of CDX2 loss with molecular features and prognosis in colorectal cancer. *Clin Cancer Res*. (2009) 15:4665–73. doi: 10.1158/1078-0432.ccr-09-0401
36. Olsen J, Eiholm S, Kirkeby LT, Espersen ML, Jess P, Gögenür I, et al. CDX2 downregulation is associated with poor differentiation and MMR deficiency in colon cancer. *Exp Mol Pathol*. (2016) 100:59–66. doi: 10.1016/j.yexmp.2015.11.009